RSC Applied Polymers

Accepted Manuscript

This article can be cited before page numbers have been issued, to do this please use: K. Shinde, S. Shinde and R. Thorave, *RSC Appl. Polym.*, 2026, DOI: 10.1039/D6LP00048G.

ROYAL SOCIETY OF CHEMISTRY

rsc.li/RSCApplPolym

View Article Online
DOI: 10.1039/D6LP00048G

ARTICLE

Tailored Imprinted Polymers for Selective Recognition of Sulfonated Dyes: Extraction of dyes from Soft Drinks, Water and Food Samples

Received 00th January 20xx,
Accepted 00th January 20xx

DOI: 10.1039/x0xx00000x

Krushna Shinde[‡a], Rupali Thorave[*‡a], and Sudhirkumar Shinde[*a]

Synthetic sulfonated food dyes in beverages and processed foods pose health and environmental risks due to their persistence and potential toxicity, whereas traditional detection methods lack selectivity and involve excessive solvent use. Here, we report synthesis of molecularly imprinted polymers (MIPs) featuring with high affinity and enhanced binding capacity for sulfonated dyes. The MIPs were prepared using phenyl sulfonic acid (PSA) as a template, a tweezer-type bis-imidazolium functional monomer, 2-hydroxyethyl methacrylate (HEMA) co-monomer, and ethylene glycol dimethacrylate (EGDMA) crosslinker. The reocgnition performance of the PSA imprinted MIPs was evaluated via rebinding isotherm data, fitted to the mono-Langmuir isotherm model revealing binding capacities ranging from 100 - 300 µmol g^{-1} with affinites in order to 10^3-10^4 M^{-1} affinity in both organic and aqueous solvents. The optimized demonstarted superior affinity for a wide range of structurally diverse sulfonated dyes containing a PSA substructure It's practical applicability was confirmed through successful recognition of commercial dyes in water, soft drinks, and food matrices, including the successful capture of adulterated food dye from turmeric samples. As a proof of concept, class-selective MIPs were employed as adsorbents in solid-phase extraction cartridges (SPE), effectively capturing trace amounts of sulfonated dyes from water. Collectively, these results underscore the potential of the developed MIPs for food monitoring and environmental remediation.

Introduction

The estimated worldwide annual production of synthetic dyes exceeds 7 x 10^5 tons. These dyes are widely utilized across diverse industries, including textile dyeing, paper, pulp, plastic, color, photographs, foods, cosmetics and other industrial applications.[1] According to Grand View Research (GVR, 2023), the global food colors market size was valued at USD 3.13 billion in 2023, and it is expected to grow at a compound annual growth rate (CAGR) of 6.5% from 2024 to 2030.[2] Synthetic food dyes, particularly sulfonated aromatic compounds and sulfonated azo dyes, are extensively used to enhance the visual appeal of beverages, confectionery, and processed foods.[3] Among these, Tartrazine (TZ, E102), Sunset Yellow (SY, E110), Carmoisine (E122), Amaranth (AM, E123), Ponceau 4R (E124), Allura Red AC (E129), Brilliant Blue (E 133), and HT Brown (E155) are the most utilized.[4, 5] The release of sulfonated azo dyes into aquatic environments has significant ecological consequences. These compounds interfere with light penetration by altering sunlight absorption and reflection, thereby disrupting photosynthetic activity and biological functioning of aquatic organisms. In addition, they can reduce dissolved oxygen levels, ultimately leading to the degradation of aquatic ecosystems. Exposure of synthetic azo dyes and degradation products such as aromatic amines, compounds classified as possible human carcinogens associated with potential health risk and overall ecological toxicity.[6] The continued application of these colorants raises concern regarding their long term safety. Regulatory agencies, including the European Food Safety Authority (EFSA) and the US Food and Drug Administration (FDA), have established guidelines to control their use and ensure consumer safety.[7, 8] Nevertheless, despite extensive research on dietary exposures and associated health risks, the data remains controversial. Acceptable intake limits have been proposed; however, certain studies emphasize the need of stricter monitoring and regulation of sulfonated dyes in food products.[9,10] Industrial wastewater containing synthetic dyes particularly from textiles and food processing industries – represent a major environmental challenge. Aromatic sulfonates are characterized by high acidity (pKa < -1), strong hydrophilicity, and low n-octanol–water partition coefficients (log K > 2.2). As a result, these compounds exhibit high mobility in the aquatic system, and pass through wastewater treatment processes.[11] Conventional wastewater treatment methods including adsorption, flocculation, coagulation, ultrafiltration, reverse osmosis and oxidation processes are inappropriate for industrial applications due to high sludge generation and cost.[12] Consequently, current physical, chemical, and biological

[a] School of Consciousness, Dr Vishwanath Karad MIT World Peace University Kothrud 411038 Pune India
‡These authors contributed equally. *Dr. Sudhirkumar Shinde, Email: sudhirkumar.shinde@mitwpu.edu.in or Dr Rupali Thorave; rupali.patil@mitwpu.edu.in (Supplementary Information available: Material, methods including the experimental procedure of rebinding experiments, HPLC methods, IR spectra, optical/fluorescence images of P1/P_N1, HPLC spectra, fitting data for the rebinding isotherm, literature survey of imprinted polymers using sulfonated dye templates) See DOI: 10.1039/x0xx00000x

View Article Online DOI: 10.1039/D6LP00018C

methods struggle to effectively remove the color from dye-containing effluents, highlighting the need for efficient, cost-effective and sustainable treatment technologies. The accurate detection and removal of dyes from foods and beverages remain a critical area of research. Several physicochemical quantification methods have many limitations due to high cost, low efficiency, high energy consumption and secondary pollution.[13, 14]

Common analytical techniques for dye detection include UV–Vis spectrophotometry and chromatographic techniques, such as thin layer chromatography (TLC), high-performance liquid chromatography (HPLC), capillary electrophoresis, liquid chromatography mass spectroscopy (LC-MS), and gas chromatography mass spectroscopy (GC-MS).[15] Although highly sensitive, these methods require efficient sample pre-treatment due to matrix interferences from soft drink components such as sugars, preservatives, and organic acids. Conventional pre-treatment strategies such as liquid–liquid extraction (LLE), solid-phase extraction (SPE), membrane extraction, and ion-exchange chromatography face challenges such as poor selectivity, high solvent usage, and limited reusability.[16] Sample treatment constitutes a critical phase that demands meticulous refinement to mitigate matrix interferences and ensure compatibility with the specific food matrix under analysis. Therefore, the development of straightforward, selective, effective pre-concentration and extraction methodologies is of paramount significance, particularly when coupled with the application of highly sensitive chromatographic and spectrometric techniques for the precise quantification of target dyes within diverse food matrices.

Molecularly imprinted polymer (MIPs) technology offers a promising approach to address these challenges. MIPs are synthetic polymers engineered with tailor-made recognition sites complementary in size, shape, and functional groups to a target molecule.[17-19] MIPs are prepared by polymerizing functional monomers and cross-linkers in the presence of a template molecule (e.g., dye). Upon removal of the template, cavities with specific binding affinity to the dye remain. Compared to biological receptors such as antibodies, MIPs have gained popularity due to their robustness, thermal and chemical stability, low cost, and reusability. MIPs have proven effective in capturing various targets, ranging from small molecules to larger entities such as pharmaceuticals and pesticides,[20, 21] peptides, proteins,[22] glycans,[23] and cells[24, 25] Nevertheless, further research is needed to explore the synthesis and application of MIPs, especially for sulfonated food dyes or sulfated biomolecules.[26-29] In recent years, sulfonated dye-selective MIPs have gained significant attention in the research community, as evidenced by numerous studies (Table S1). These polymers are synthesized using broad range of sulfonated dye templates, including Acid Black 1, Acid Black 210, Acid Brown 703, Acid Green 16, SY, Acid Violet 19, Cibacorn Red Dye, Direct Red 23, TZ, and Congo Red (CR). Researchers have investigated a variety of neutral and cationic charged functional monomers, such as acryloyloxyethyl trimethyl ammonium chloride, methacrylic acid, 1-(α-methyl acrylate)-3-methylimidazolium bromide, acrylamide, 1-vinyl imidazole, 3-aminopropyltrimethoxysilane, and titanium isopropoxide. These functional monomers play a key role in the interactions between the sulfonated groups of dye templates in the pre-polymerization stage and in stabilizing the monomer-template complex throughout polymerization, which ultimately shapes the binding sites within the MIPs structure. Polar solvents, or their mixtures, are often preferred, particularly when sulfonated dyes act as templates, as this promotes stable pre-polymerization complexes – a pre-requisite for generating well-defined and effective recognition sites. The effectiveness of MIPs is typically evaluated by comparing their performance against non-imprinted polymers (NIPs). Studies (Table S1) consistently show that MIPs exhibit higher dye-binding capacities and selectivity than NIPs. This enhanced functionality makes them particularly well-suited for various applications, especially the removal of dyes from contaminated water sources. Dye-specific MIPs have been successfully used to bind and remove imprinted dyes from wastewater, river water, and industrial discharge. Despite these advantages, sulfonated dyes present several limitations when used as templates for synthesizing MIPs, including the introduction of additional environmental burden. The removal of the template from the polymer generates non-environmentally friendly solvent waste. Another common technical issue arises from the use of protic polar solvents, which, while required to dissolve sulfonated dyes, can detrimentally impact monomer-template complexation when employed as a porogen. Specific sulfonated dye imprinted materials, while effective for targeted dyes, often lack versatility due to their limited selectivity. To address these challenges, this study introduces a novel approach by creating class-selective MIPs designed for the general recognition of dyes containing phenyl sulfonate moieties. Phenyl sulfonic acid (PSA) is employed as a substructure template due to its non-toxic nature, cost-effectiveness, and prevalence structure in commercial sulfonated dyes. This study systematically explores the influence of polymer compositions and azo initiators on the molecular recognition, binding affinity, and binding capacity of templates, focusing on sulfonated dyes containing the PSA moiety. A comprehensive examination of the MIPs' recognition capabilities is conducted in both pure water and polar environments containing potential interfering compounds, providing a thorough assessment of their selectivity and robustness. The applicability of the developed MIPs is demonstrated through successful recognition and extraction of target sulfonated dyes from water, food samples, and soft drink samples, showcasing their potential for practical, real-world applications.

Experimental

Materials

Tetrabutylammonium hydroxide (TBAOH; 10% in methanol) and 95% ammonium hexafluoro phosphate (NH_4PF_6) was received from Sisco Research Laboratory (SRL) India.

phenylsulfonic acid (PSA) were purchased from Avra Synthesis Private Limited India. EGDMA and HEMA were received from Otto Chemie Pvt Ltd India. 1-vinylimidazole (> 98%) was received from TCI Japan. N,N'-Azo-bis(2,4-dimethyl) valeronitrile (ABDV) was received from Simson Pharma Limited India. Dry MeCN was received from Merck USA. Sodium benzyl Orange (Na-BO) was received from TCI, Japan. 2% TZ was received from Garden Flavours Company Pvt. Ltd. 6% SY was received from Bakers Ville India Pvt. Ltd., Alizarin Red S (AR), and Metanil Yellow (MY), Fast Green FCF (FG), AM, and Indigo Carmine (IC) were received from Otto Chemie Pvt. Ltd. India. Methyl Orange (MO) Methylene blue (MB) was received from TCI, Japan. 37% hydrochloric acid (HCl) was received from Merck Life Sciences India. HPLC grade 99.8% trifluoroacetic (TFA), HPLC grade methanol, HPLC grade MeCN, sodium chloride (NaCl) and 25% NH_3 solution was received from Loba Chemie Pvt. Ltd. India. Glacial Acetic acid was received from Clairo Filt India. The Functional monomer 1-Vinyl-3-{3-[(1-vinyl-1H-imidazol-3-ium-3-yl)methyl]benzyl}-1H-imidazol-3-ium bishexafluorophosphate (FM, $1^{2+}.2PF_6^-$) was synthesized according to a previously reported procedure.[29] EGDMA and HEMA were passed through a column of activated basic alumina to remove inhibitors and stored at - 20 °C before polymerization.

Synthesis of Imprinted Polymers (P1, P2, P_N1, P_N2)

The imprinted polymer P1 was prepared by dissolving the template TBA PSA (0.2 mmol; 79.7 mg) and the functional monomer 1^{2+} $2PF_6^-$ (0.2 mmol; 116.5 mg) complex in 1120 μL of dry MeCN. EGDMA (755 μL; 4 mmol) was added as a crosslinker to this monomer–template complex solution. For the imprinted polymer P2, a complex was formed by dissolving the template TBA PSA (0.4 mmol; 159.5 mg) and the functional monomer 1^{2+} $2PF_6^-$ (0.4 mmol; 227.5 mg) in 2240 μL of dry MeCN. The co-monomer HEMA (1.6 mmol; 195 μL) and EGDMA crosslinker (455 μL; 2.4 mmol) were added to the functional monomer template complex solution. For each polymer, 10 mg of the ABDV initiator was added to the above 10 mL screw-capped sintered vials containing the pre-polymerization solution. The solution was purged with a flow of dry nitrogen at room temperature for 5 min. The vials were closed with a lid and then sealed with silicone tape. Then, polymerization was carried out at 48°C for 24 h in a preheated oven. After polymerization, the glass vials were broken, and the bulk polymers were crushed into coarse particles. The template was removed from the polymers by shaking overnight in 1 N HCl, and again washed in 2 h in the 1 N HCl, then 1 h in the 50 mL methanol: acetic acid: water/85:15:5 (v/v) solvent mixture, followed by two times with 50 mL of distilled water and a final washed with 50 mL of HPLC-grade methanol. The polymer was then dried in the oven at 40°C for 2 h and thereafter subjected to fine grinding with a mortar and pestle to achieve particle size of 10 µm - 500 µm. The obtained particles, without sieving, were used to assess the binding properties. Reference polymers named non-imprinted polymer NIPs (P_N1 and P_N2) corresponding to imprinted polymers with different proportions of imprinted polymers were prepared as described above, but in the absence of the template molecule from the pre-polymerization solution.

Results and discussion

View Article Online
DOI: 10.1039/D6LP00048G

Table 1. Polymer Composition of PSA-Imprinted Polymers Prepared by Azo-Initiated Thermal Polymerization in Dry Acetonitrile.

Polymer	Template (T, mmol)	Functional Monomer (FM, mmol)	Comonomer (CM, mmol)	Crosslinker (CL, mmol)	Porogen (mL)
P1	TBA PSA (0.2)	$1^{2+}.2PF_6^-$ (0.2)	-	EGDMA (4)	MeCN (1.12 mL)
P_N1		$1^{2+}.2PF_6^-$ (0.2)	-	EGDMA (4)	MeCN (1.12 mL)
P2	TBA PSA (0.4)	$1^{2+}.2PF_6^-$ (0.4)	HEMA (1.6)	EGDMA (2.4)	MeCN (2.24 mL)
P_N2		$1^{2+}.2PF_6^-$ (0.4)	HEMA (1.6)	EGDMA (2.4)	MeCN (2.24 mL)

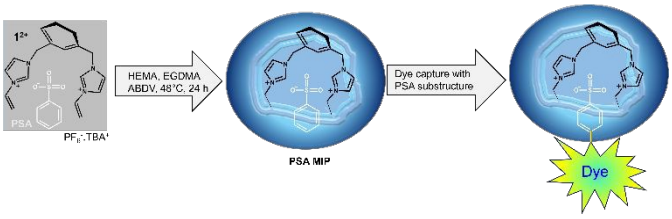

Figure 1. Depiction of PSA recognition cavity in imprinted receptor and principle of capture dye containing PSA substructure. PSA MIP made from complex of tweezer type imidazolium functional monomers ($1^{2+}.2PF6^-$: FM) and TBA PSA template in presence of HEMA comonomer (CM), EGDMA crosslinker (CL) and ABDV initiator at 48 °C

In a prior investigation, a unique tweezer-type dipodal functional monomer (FM) featuring imidazolium groups at the 1,3 positions of benzene rings and terminal vinyl polymerizable groups (illustrated in Figure **1**, $1^{2+}.2PF_6^-$), demonstrated significant interactions with sulfonates in acetonitrile. Thorave *et. al.* reported the association constants (*Ka*) of the $1^{2+}.2PF_6^-$-:TBA PSA (FM:T) complex to be 6.17 x 10^3 M^{-1} and 3.7 x 10^3 M^{-1} as determined by UV and ^1H NMR titration at room temperature respectively.[29] In our previous report, the stoichiometric complex, comprising TBA PSA and $1^{2+}.2PF_6^-$, was utilized in the production of MIPs using an EGDMA crosslinker, both with and without the incorporation of a HEMA comonomer.[29] These polymers were synthesized via thermal polymerization in MeCN solvent using AIBN initiator at 65°C. Based on our previous findings, incorporating the water-loving HEMA comonomer into MIPs improves their water compatibility and enhances their ability to bind larger analytes containing phenyl sulfonate substructures. Azobisisobutyronitrile (AIBN) and ABDV are thermal azo initiators commonly used in free radical polymerization in organic solvents. ABDV is better suited for lower-temperature polymerization due to its lower decomposition temperature; its 10-hour half-life temperature

View Article Online
DOI: 10.1039/D5LP00048C

is 51°C, compared to 65°C for AIBN. The polymerization temperature is expected to substantially influence the

Table 2. The binding constants (Ka) and specific binding capacities (Bmax) for polymers P1, P_N1, P2, P_N2 from the rebinding isotherm were obtained using TBA PSA in 100% MeCN and PSA and TZ in 100% H_2O.

Polymer: Analyte	Rebinding Solvent	Ka (x 10^3 M^{-1})	B_{max} (µmol g^{-1})	Ref Figure (SI)
P1: TBA PSA	100% MeCN	12.77	99.69 ± 20.14	Fig S2
P_N1: TBA PSA		7.93	77.37 ±12.9	
P2: TBA PSA		**23.81**	**118.1 ± 18.15**	
P_N2: TBA PSA		15.72	78.8 ± 11.16	
P1: PSA	100% H_2O	21.21	247.1 ± 18.1	Fig S4
P_N1: PSA		23.36	168.1 ± 7.45	
P2: PSA		**15.89**	**309.4 ± 31.05**	
P_N2: PSA		20.70	175.1 ± 9.6	
P2: TZ	100% H_2O	24.27	129.2 ± 22.8	Fig 3
PN2: TZ		21.94	66.56 ± 15.98	

polymer's affinity and specificity, thereby affecting the monomer-template complex and the polymerization process. Building on these prior results, the present study explores the polymerization of the $1^{2+}.2PF_6^-$: TBA PSA complex combined with the EGDMA crosslinker, either with or without the HEMA comonomer, using the azo-initiator ABDV at 48 °C for 24 h in a conventional oven. Inspired by the growing field of metal-organic framework-derived porous functional polymers[30] and considering bis-imidazolium functional monomers provides additional crosslinking density, the polymer composition was optimized by reducing the crosslinker concentration and increasing the monomer-template complex concentration, as detailed in Table 1. Both PSA-imprinted polymers (P1, P2) and reference polymers synthesized without TBA PSA and designated as non-imprinted polymers (P_N1, P_N2), were produced. The resulting polymers were processed into particulate form through manual grinding with a mortar and pestle, followed by extensive washing with a 1N HCl, acidic methanol, water, and methanol to eliminate any residual unreacted monomers and templates. Optical microscopy and IR spectroscopy (Figure S1) were employed to confirm the polymers identities and ensure comparable morphology and composition. Subsequently, rebinding assays were conducted to assess the polymers' recognition capabilities toward the TBA PSA. Polymers were incubated in MeCN containing varying concentrations of TBA PSA (ranging from 0 to 5 mM), and the level of unbound analyte in the supernatant were quantified using HPLC-UV (Figure S2).

The amount of TBA PSA bound to the polymers was then calculated using Equation S1. A Langmuir monosite binding model was applied to the data presented in Figure S2 (Equation S2) allowing estimation of binding constants (*Ka*) and capacity (Bmax). The fitting data, shown in Figure S2 and summarized in Table 2, revealed an affinity (Ka) of P1 for the class 1 binding sites of 12.77 x 10^3 M^{-1}, which is 1.61 times greater than that of P_N1 (Ka = 7.93 x 10^3 M^{-1}). The binding capacities (Bmax) of P1 and P_N1 were determined as 99.69 ± 20.14 µmol g^{-1} and 77.37 ± 12.95 µmol g^{-1}, respectively. As depicted in Figure 1, the imprinted polymer P1, featuring its PSA-specific cavities, exhibited superior affinity for TBA PSA, whereas the non-imprinted polymer P_N1 displayed lower affinity, confirming the successful imprinting of PSA within the imprinted polymers. The enhanced affinity of P1 underscores the effectiveness of the imprinting process in creating selective binding sites for the target analyte. In this study, we evaluated the imprinting capabilities of P1/P_N1 (Figure S2) and RP1/RP_N1 polymers (Figure S3), which were synthesized using azo initiators at polymerization temperature of ABDV and AIBN[29] at 48°C and 65°C, respectively. Our findings indicate that the RP1/RP_N1 polymer, synthesized with AIBN, exhibited a slightly lower imprinting effect (*Ka* – 9.36 x 10^3 M^{-1}) compared to the P1/P_N1 polymers (Table 2). This observation aligns with the principle that the interaction strength between the imidazolium cation of the functional monomer and sulfonate-based anions, primarily facilitated by hydrogen bonding, exhibits an inverse relationship with temperature.[31] The results are consistent with previous studies indicating that reduced polymerization temperatures promote the formation of monomer-template complexes and the synthesis of MIPs through hydrogen bonding and electrostatic interactions, thereby influencing the characteristics and number of MIPs recognition sites.[32, 33] The rebinding isotherm data, analyzed using a one-site binding model for TBA PSA (Figure S2 and Table 2), revealed a binding affinity (*Ka*) of 23.81 x 10^3 M^{-1} for P2. This value represents a 1.51-fold increase compared to the *Ka* observed for P_N2 (15.72 x 10^3 M^{-1}). Interestingly, the binding capacity (Bmax) for both NIPs, P_N1 and P_N2, remained consistent at approximately 78 ± 11.2 µmol g^{-1}, indicating comparable saturation levels of bound analyte. However, a notable enhancement in binding capacity was observed for P2 (118 ± 18.15 µmol g^{-1}) when compared to P1. These findings suggest that polymer P2 and P_N2, characterized by a higher concentration of the monomer-template complex exhibit superior binding characteristics, leading to improved affinity and capacity for the TBA PSA. Polymer compositions of P2/P_N2 incorporating the template-functional monomer (T:FM) complex were synthesized with a T:FM:CM:CL ratio of 2:2:12:8 (in mmol). This represents a doubling of the T:FM ratio compared to previous polymers that were T:FM:CM:CL ratio of 1:1:12:8 (in mmol).[29] The T:FM ratio is also significantly higher than that of polymer P1/P_N1, which has a FM:T:CL ratio of 1:1:20 (in mmol) as shown in Table 1. The

enhanced binding capacity in P2 (Table 2) suggests a higher concentration of monomer-template complex, potentially generates a greater number of recognition sites.

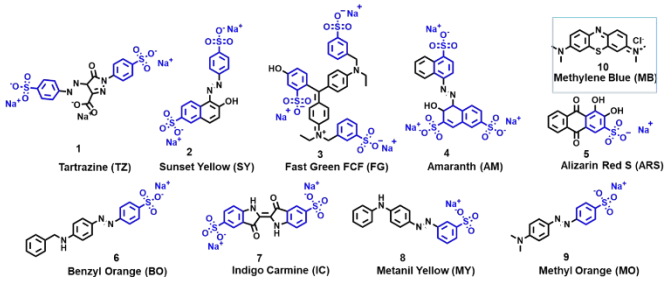

Figure 2. Chemical structure of sulfonated dyes (1 to 9) containing PSA moiety and control dye (10) without sulfonate group, used for the evaluation of P2, P_N2 polymers.

Following the successful imprinting of TBA PSA in MeCN, the study assessed polymer recognition of the PSA analyte in 100% water. As summarized in Table 2 and Figure S4, all polymers demonstrated a binding affinity of roughly 2 x 10^4 M^{-1}. Polymer P2 exhibited a higher binding capacity for PSA (Bmax - 309.4 ± 30.25 µmol g^{-1}) than P1 (Bmax - 247.1 ± 18.1 µmol g^{-1}).

The water-soluble synthetic azo dye, SY, which contains phenyl sulfonate moieties, was examined for its interaction with P2 and P_N2 polymer particles. Briefly, 5 mg of each polymer was incubated in 4 ml of water containing 0.1 mM of the SY dye for 15 min. After removing the supernatant and washing with acidic and basic solvents, optical and fluorescence images were taken using a red excitation filter and an exposure time of 700 ms. Figure S5 displays fluorescence images revealing a significant difference in fluorescence intensity between P2 and P_N2 particles. P2 particles exhibited strong fluorescence, suggesting substantial SY retention. Conversely, P_N2 particles exhibited weak fluorescence, indicating a lower affinity for SY than imprinted polymer P2. The washing fractions were collected, and the combined fractions were quantified by HPLC-UV spectroscopy. The results were consistent with the fluorescence measurements, confirming that the imprinted polymer P2 retained ≥65% of the SY, whereas the non-imprinted polymer P_N2 retained only approximately 33%.

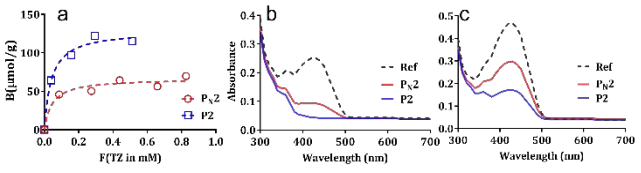

Figure 3. (a) Rebinding isotherm of TZ dye with P2 and P_N2 polymers in 100% water. Absorbance spectra of the supernatant after rebinding of TZ dye (1 mL) with 2.5 mg of polymer at concentrations of (b) 0.2 mM and (c) 0.4 mM TZ in 100% water.

Based on preliminary data indicating improved selectivity of the produced imprinted polymer for SY dye, a quantitative examination of binding affinity and capacity was performed using TZ dye in an aqueous medium. TZ dye was selected as a suitable analyte for the rebinding experiments dues to its structural features, particularly the presence of two phenyl sulfonate moieties, which are expected to interact favorably with the binding sites in the imprinted polymer matrix. In the rebinding experiments, polymer P2 and P_N2 were accurately weighed (2.5 mg each) and suspended in 1 mL of TZ dye solutions. A range of TZ dye concentrations spanning from 0 to 2 mM was prepared to generate a comprehensive rebinding isotherm. The suspensions were gently agitated on a shaker at room temperature for a duration of 100 min to ensure equilibrium. Following the incubation period, the samples were centrifuged at 10000 rpm for 5 min to separate the polymer particles from the supernatant. The supernatant was carefully collected and dye compared to P_N2 and the reference sample.

To quantify the amount of TZ dye bound to the polymers, a rebinding isotherm was constructed (Figure 3a). The isotherm was plotted with bound TZ (µmol g^{-1}) versus free TZ concentration fitting with one site binding model (Equation S2). The concentration of TZ dye remaining in the supernatant was determined by measuring the absorbance at 430 nm using an external calibration curve. Rebinding analysis revealed similar affinity constants (*Ka*) of approximately 2 x10^4 M^{-1} for both P2 and P_N2. However, the binding capacity of P2 (129.2 ± 22.8 µmol g^{-1}) was roughly twice that of P_N2 (Table 1), suggesting that the imprinting process significantly enhanced TZ binding capacity of P2.

Sulfonated dyes shown in Figure 2 include TZ (**1**), SY (**2**), FG (**3**), AM (**4**), AR (**5**), BO (**6**), IC (**7**), MY (**8**), and MO (**9**), all of which contain one, two, or three phenyl sulfonate moieties. These dyes were subjected to single point rebinding assays, a design chosen to demonstrate the broad utility of MIPs for capturing

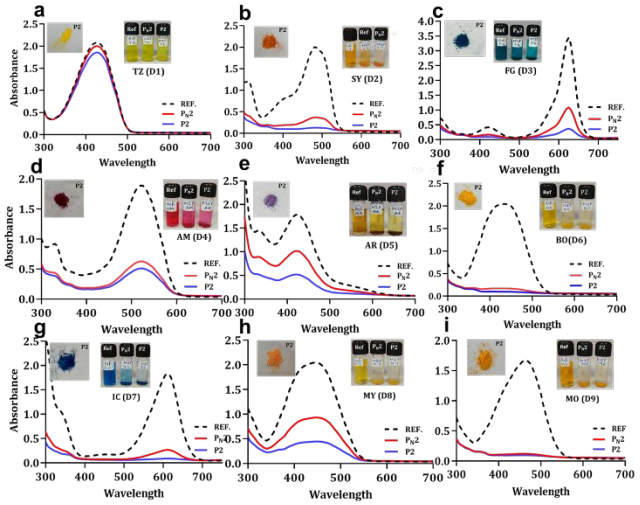

Figure 4. Binding of sulfonated dyes by P2, P_N2 in 100% water. Absorption spectra of (a) TZ, (b) SY, (c) FG, (d) AM, (e) AR, (f) BO, (g) IC, (h) MY, and (i) MO, after incubation with P2, P_N2, along with reference spectrum of each dye solutions. Inset: Photographs of dye binding experiment in glass vials after 20 min, showing P2 polymers with captured dyes.

sulfonated dyes bearing the template substructure. Methylene blue (MB, **10**) which lacks a phenyl sulfonate substructure, was included as a control. P2/P_N2 polymers (5 mg) were dispersed

View Article Online
DOI: 10.1039/D6LP00048G

in 4 mL of aqueous solutions containing individual dyes at concentrations of 1 mM for TZ, AR, and MY and 0.1 mM for SY, FG, AM, BO, IC, and MO. After a 15-min settling period, 300 µL of the supernatant was analyzed using a multiplate reader (BioTek Synergy H) over a wavelengths range of 230 to 900 nm. Absorbance spectra (Figure 4a – 4i) showed that P2 polymers exhibited higher dye uptake compared to both P_N2 polymers and the reference dye solution, as evidenced by the lower intensity of the P2 supernatant and visually confirmed by images of the dye-bound P2 polymer (Inset Figure 4a – 4i). In contrast, no significant differences were observed between P2, P_N2, and the reference MB dye solution (Figure S6), with no visible changes in the supernatant solutions or dye-bound polymers.

Polymer P2 and P_N2 were subsequently evaluated direct interaction with sulfonated dyes in a selection of commercially available beverages. This set comprised five distinct commercial

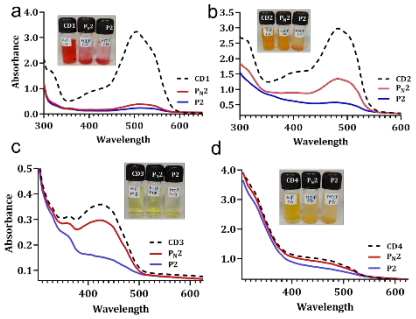

Figure 5. Sulfonate dye binding by P2, P_N2 in soft drink CD1 - CD4. Absorption spectra of (a) CD1, (b) CD2, (c) CD3, and (d) CD4 after polymer treatment, reference spectra of the original soft drinks. Inset: photographs of dye binding experiment in glass vials after 25 min.

drinks (Figure S7): three carbonated beverages (CD1, CD2, CD3) and two fruit juices (CD4, CD5). The tested beverages contained mixture of sugars and additives, including artificial sweeteners, flavorings, and preservatives, alongside the target sulfonated dyes. Notably, CD1 and CD3 contained caffeine at concentrations of 29 and 13 mg per 100 mL, respectively. The fruit juices, CD4 and CD5 consisted of 10.5% orange juice from pulp and 5.1% concentrate mango pulp, respectively. The specific sulfonated dyes present were: Allura red CD1, SY CD2, TZ CD3, a combination of TZ and SY CD4, and SY CD5. Briefly, P2/P_N2 polymers (11 mg CD1, 5 mg CD2, 1 mg CD3, and 2.5 mg CD4, CD5) were suspended in 4 ml of each soft drinks, incubated for 15 min, and analyzed by UV-Vis spectroscopy (230-900 nm). These spectra were compared with those of P_N2 and the original soft drinks. The UV spectra (Figure 5a, 5b, 5c, 5d and Figure S8) revealed that the polymer P2 adsorbed dyes from soft drinks to a greater extent than P_N2 and the reference drinks. Obvious visual differences among P2, P_N2, and soft drinks were also captured in the inset photographs of Figure 5. These results indicate that MIPs can selectively recognize sulfonated dyes in the complex matrix of soft drink matrices where high polarity and interferences from sugar, organic acids, and preservative are present.

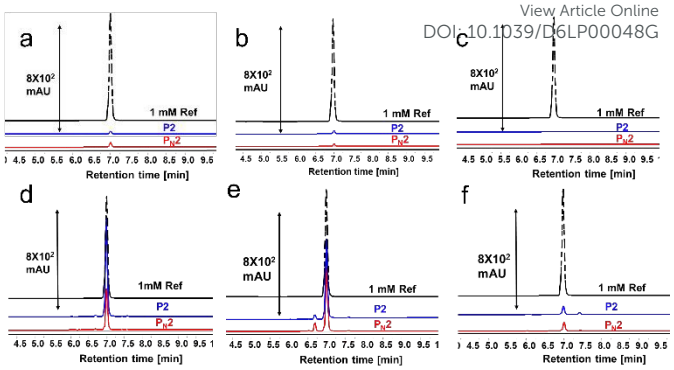

Figure 6. C18-HPLC-UV spectra of eluted fractions of P2, and P_N2 afte MYr dye extraction from three turmeric samples. **Elution fraction 1**: (a) sample 1 (b) sample 2, (c) sample 3 and **elution fraction 2**: (d) sample 1, (e), sample 2, (f) sample 3. In each panel, the spectra from P2 and P_N2 are overlaid for direct comparison.

MY an unapproved food colorant worldwide[34] belongs to yellow azo dye class and finds diverse applications in the wool, silk, paper ink, and aluminum industries. Despite its industrial versatility, MY consumption poses significant health risks. Studies have linked MY exposure to neurotoxicity, carcinogenicity, and genotoxicity, as harmful effects on critical organs such as the brain, liver, kidneys, testes, and ovaries.[35] Concerns have been raised about its presence in food products, particularly turmeric, especially those processed by unorganized sectors. To investigate the presence of MY, four samples of non-food grade turmeric powder were collected from local markets. Sample preparation involved dissolving 200 mg of turmeric powder into 10 mL of water. Following this, 1 mL of the supernatant solution was used for MY dye extraction using 2 mg of P2/P_N2 polymer. After washing with acidic and basic solvents, two elution fractions were dried by evaporation and reconstituted in water. The extracted MY dye was analyzed by C18-HPLC-UV method. Analysis of HPLC spectra from eluted fractions (Figure 6), coupled with the quantified MY dye data (Table S2), demonstrated that the P2 polymer displayed a superior binding affinity for MY dyes extracted from the collected samples compared to P_N2. MY was detected in three

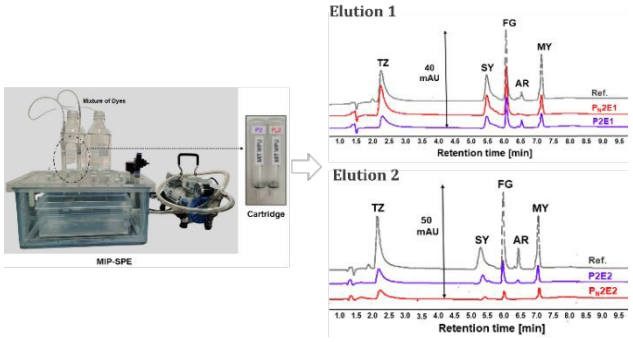

Figure 7. (a) MIP-SPE units with P2, P_N2 cartridges. (b) C18-HPLC-UV chromatograms of eluted fractions (E1, E2) from P2, P_N2 cartridges after extraction of a dye mixture (TZ, SY, FG, AR, and MY; 4.5 x10^{-8} M in 1L water. Ref: dye mixture in elution solvent. Peaks are labelled with dye names.

View Article Online
DOI: 10.1039/D6LP00048G

of four turmeric samples at concentrations ranging from 0.7 to 9 mg per gram of turmeric (Table S2). Sample 4 showed no detectable MY (Figure S9).

As a proof of concept, the effectiveness of synthesized MIPs for the dye extraction from water was evaluated using P2 and P_N2 as solid phase extraction (SPE) sorbents. For MIP-SPE, 20 mg of P2/P_N2 polymers were packed into 3 mL cartridges (Figure 7). An equimolar mixture of TZ, MY, FG, AR, and SY dyes (each at 45 nM) was spiked in 1 L of water. The water containing mixture of mono-, di-, and tri- sulfonated dyes was passed through the P2/P_N2 cartridges at a flow rate of 2.5 mL min^{-1} under a vacuum of approximately 30 mm Hg. After drying the polymer, adsorbed dyes were eluted in two steps (E1, E2) using acidic methanol. The eluted fractions were quantified via C18-HPLC-UV and compared with reference samples. As shown in Figure S10, the combined elution fractions for both MIP and NIP exhibited similar adsorption abilities for water-soluble dyes with a slight preference for multi-sulfonated over mono-sulfonated dyes, yielding recoveries ranging from 50% to 90% in water. Notably, the chromatograms (Figure 7) revealed higher dye concentrations in the E2 fractions from P2 compared to P_N2 in contrast to E1 fractions. This suggests that P2 polymers retain sulfonated dyes more strongly than corresponding NIPs.

Conclusions

In this study, we have developed class-selective molecularly imprinted polymers (MIPs) for the recognition of sulfonated dyes using a substructure imprinting approach with phenyl sulfonic acid (PSA) as the template and a tweezer-type bis-imidazolium functional monomer. The optimal conditions—lower polymerization temperature (48 °C) with ABDV initiator and a higher template-to-monomer ratio (P2 formulation)—markedly enhanced binding capacity and affinity. MIPs created using HEMA and EGDMA with optimized compositions demonstrated improved water compatibility compared to MIPs synthesized without HEMA. Notably, the optimized polymer (P2) demonstrated a binding capacity of 300 µmol g^{-1} and affinity constant (Ka) of 1.6 x 10^4 M^{-1} for PSA and for a structurally diverse sulfonated dyes (including TZ, SY, FG, AM, ARS, BO, IC, MY and MO) in both organic and aqueous solvent. These MIPs successfully recognized and bound sulfonated dyes even in complex matrices such as commercial soft drinks containing carbohydrates, organic acids, preservatives, and caffeine. Importantly, we have demonstrated for the first time that imprinted polymers can be used to capture adultered food dyes from turmeric samples, highlighting their potential application in food safety monitoring. As a proof of concept, developed MIPs were employed as adsorbents in solid phase extraction (SPE) cartridges, enabling the capture of a mixture of ultra-traces sulfonated dyes from water.

Collectively, these findings establish that substructure-imprinted MIPs offer a promising, selective, and robust platform for the extraction and preconcentration of sulfonated dyes from complex food and environmental matrices, with significant implications for public health protection and environmental monitoring.

Author contributions

The manuscript was written through the contributions of all authors. All authors approved the final version of the manuscript. ‡These authors contributed equally.

Conflicts of interest

There are no conflicts to declare.

Data availability

Supporting data is available in the Supplementary Information, including experimental details (materials, methods, HPLC), additional references (10) for imprinted polymers targeting sulfonated dyes (Table 2), IR (Figure S1), optical microscopy images (Figure S5), rebinding isotherms and fitting data (Figures S2-S4), and additional supporting evidence like UV and HPLC spectra (Figures S6-S10).

Acknowledgements

We highly acknowledge the financial support from Prof. Dr. Vishwanath Karad for providing a starting research grant to the School of Consciousness, Dr. Vishwanath Karad MIT World Peace University Kothrud Pune, India.

References

1. R. Al-Tohamy, S. S. Ali, F. Li, K. M. Okasha, Y. A. G. Mahmoud, T. Elsamahy, H. Jiao, Y. Fu and J. Sun, *Ecotoxicol. Environ. Saf.*, 2022, **231**, 113160.
2. GVR (2023) online https://www.grandviewresearch.com/industry-analysis/food-colorants-market.
3. P. Barciela, A. Perez-Vazquez and M. A. Prieto, *Food. Chem. Toxicol.*, 2023, **178**, 113935.
4. S. I. Kaya, A. Cetinkaya and S. A. Ozkan, *Food. Chem. Toxicol.*, 2021, **156**, 112524.
5. O. I. Lipskikh, E. I. Korotkova, Y. P. Khristunova, J. Barek and B. Kratochvil, *Electrochim. Acta.*, 2018, **260**, 974-985.
6. T. Li, L. Wei, Y. Fang, Y. Cui, X. Wang and Y. Li, *Environ. Pollut.*, 2025, **386**, 127180.
7. A. Lehmkuhler, M. D. Miller, A. Bradman, R. Castorina, M.-A. Chen, T. Xie and A. E. Mitchell, *J. Food. Compos. Anal.*, 2022, **112**, 104649.
8. N. Martins, C. L. Roriz, P. Morales, L. Barros and I. C. F. R. Ferreira, *Trends. Food. Sci. Technol.*, 2016, **52**, 1-15.
9. P. Amchova, H. Kotolova and J. Ruda-Kucerova, *Regul. Toxicol. Pharmacol.*, 2015, **73**, 914-922.
10. E. K. Dunford, T. M. Galligan, L. S. Taillie and A. A. Musicus, *J. Acad. Nutr. Diet.*, 2025, **125**, 1207-1217.e1209.
11. R. Loos and R. Niessner, *J. Chromatogr. A.*, 1998, **822**, 291-303.

View Article Online
DOI: 10.1039/D6LP00048G

12. A. Ahmad, S. H. Mohd-Setapar, C. S. Chuong, A. Khatoon, W. A. Wani, R. Kumar and M. Rafatullah, *RSC Adv.*, 2015, **5**, 30801-30818.
13. Y. Shi, Z. Yang, L. Xing, X. Zhang, X. Li and D. Zhang, *World J. Microbiol. Biotechnol.*, 2021, **37**, 137.
14. S. Dutta, B. Gupta, S. K. Srivastava and A. K. Gupta, *Mat. Adv.*, 2021, **2**, 4497-4531.
15. K. Yamjala, M. S. Nainar and N. R. Ramisetti, *Food. Chem.*, 2016, **192**, 813-824.
16. O. S. Salami, M. Sihlahla, B. S. Dladla and N. Mketo, *Trends. Food. Sci. Technol.*, 2025, **160**, 104991.
17. B. Sellergren, *TrAC Trends. Anal. Chem.*, 1997, **16**, 310-320.
18. B. Sellergren, *Molecularly imprinted polymers man-made mimics of antibodies and their applications in analytical chemistry*, Elsevier Amsterdam, 1st edn., 2000.
19. D. A. Gkika, A. K. Tolkou, D. A. Lambropoulou, D. N. Bikiaris, P. Kokkinos, I. K. Kalavrouziotis and G. Z. Kyzas, *RSC Appl. Poly.*, 2024, **2**, 127-148.
20. C. Alexander, H. S. Andersson, L. I. Andersson, R. J. Ansell, N. Kirsch, I. A. Nicholls, J. O'Mahony and M. J. Whitcombe, *J. Mol. Recognit.*, 2006, **19**, 106-180.
21. J. J. BelBruno, *Chem. Rev.*, 2019, **119**, 94-119.
22. B. Tse Sum Bui, A. Mier and K. Haupt, 2023, **19**, 2206453.
23. P. Li and Z. Liu, *Chem. Soc. Rev.*, 2024, **53**, 1870-1891.
24. S. Piletsky, F. Canfarotta, A. Poma, A. M. Bossi and S. Piletsky, *Trends. Biotechnol.*, 2020, **38**, 368-387.
25. F. Ding, Y. Ma, W. Fan, J. Xu and G. Pan, Trends Biotechnol., 2024, 42, 1097-1111.
26. S. Ambrosini, M. Serra, S. Shinde, B. Sellergren and E. De Lorenzi, *J. Chromatog. A.*, 2011, **1218**, 6961-6969.
27. S. Shinde, A. Bunschoten, J. A. W. Kruijtzer, R. M. J. Liskamp and B. Sellergren, *Angew. Chem, Int. Ed.* , 2012, **51**, 8326-8329.
28. S. Shinde, A. Incel, M. Mansour, G. D. Olsson, I. A. Nicholls, C. Esen, J. Urraca and B. Sellergren, *J. Am. Chem. Soc.*, 2020, **142**, 11404-11416.
29. R. Thorave, M. Celentano, K. Bankar, B. Sellergren, P. Manesiotis and S. A. Shinde, *Polymer. Sci. Technol.*, 2025, **1**, 488-499.
30. S. K. Firooz and D. W. Armstrong, *Anal. Chim. Acta.*, 2022, **1234**, 340208.
31. N. R. Pitawela and S. K. Shaw, *ACS Meas. Sci. Au.*, 2021, **1**, 117-130.
32. Y. Lu, C. Li, X. Wang, P. Sun and X. Xing, *J. Chromatogr. B.*, 2004, **804**, 53-59.
33. E. V. Piletska, A. R. Guerreiro, M. J. Whitcombe and S. A. Piletsky, *Macromolecules*, 2009, **42**, 4921-4928.
34. I. S. Khan, M. N. Ali, R. Hamid and S. A. Ganie, *Toxicol. Rep.*, 2020, **7**, 370-375.
35. T. N. Nagaraja and T. Desiraju, *Food. Chem. Toxicol.*, 1993, **31**, 41-44.

View Article Online
DOI: 10.1039/D6LP00048G

Data Availability Statement

Dear Editor,

Supporting data is available in the Supplementary Information, including experimental details (materials, methods, HPLC), additional references (10) for imprinted polymers targeting sulfonated dyes (Table 2), IR (Figure S1), optical microscopy images (Figure S5), rebinding isotherms and fitting data (Figures S2-S4), and additional supporting evidence like UV and HPLC spectra (Figures S6-S10).

Yours faithfully,

Prof. Sudhirkumar Shinde, *Ph.D.*

Associate Professor,

Dr Vishwanath Karad MIT World Peace University Pune India.